Aluminum methylamidoborane complexes: mechanochemical synthesis, structure, stability and reactive hydride composites

Ting Zhang, Timothy Steenhaut, Xiao Li, François Devred, Michel Devillers *, and Yaroslav Filinchuk *

$$CH_3NH_2{\cdot}HCl + NaBH_4 \longrightarrow CH_3NH_2BH_3 + NaCl + H_2\uparrow \quad (1)$$

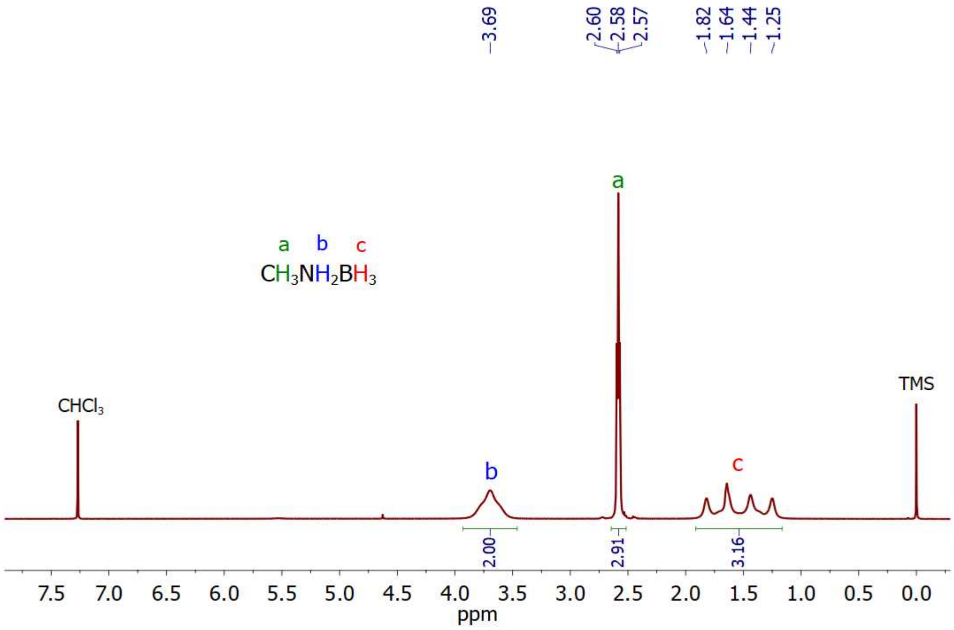

Fig. S1 ^{1}H NMR spectrum of $CH_3NH_2BH_3$

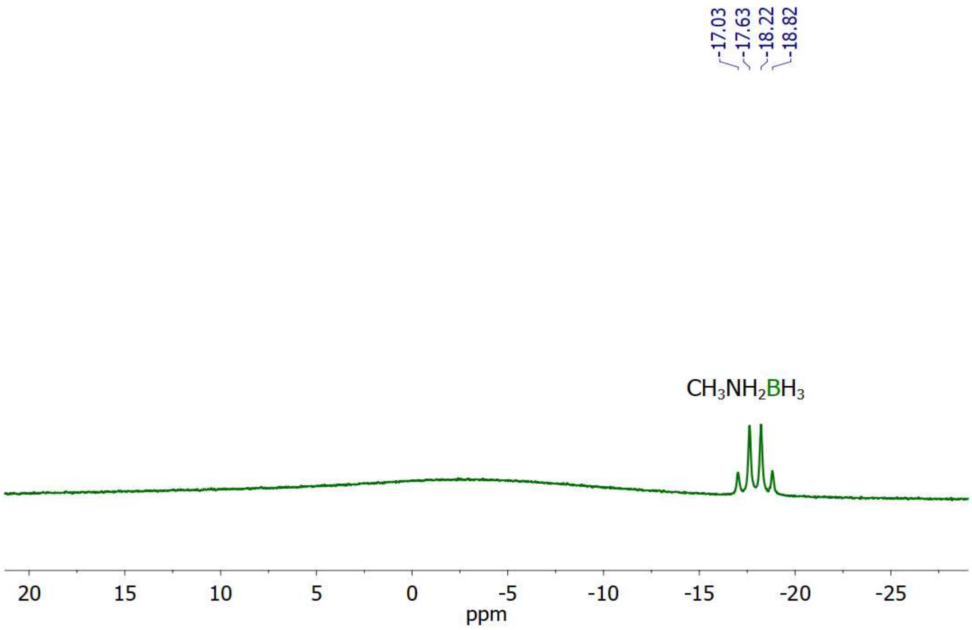

Fig. S2 ^{11}B NMR spectrum of $CH_3NH_2BH_3$

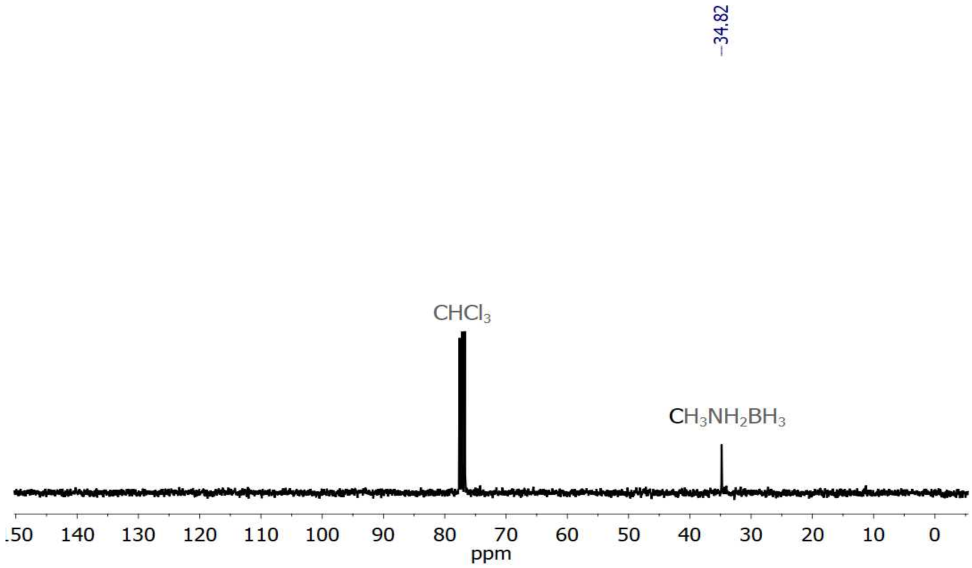

Fig. S3 ^{13}C NMR spectrum of $CH_3NH_2BH_3$

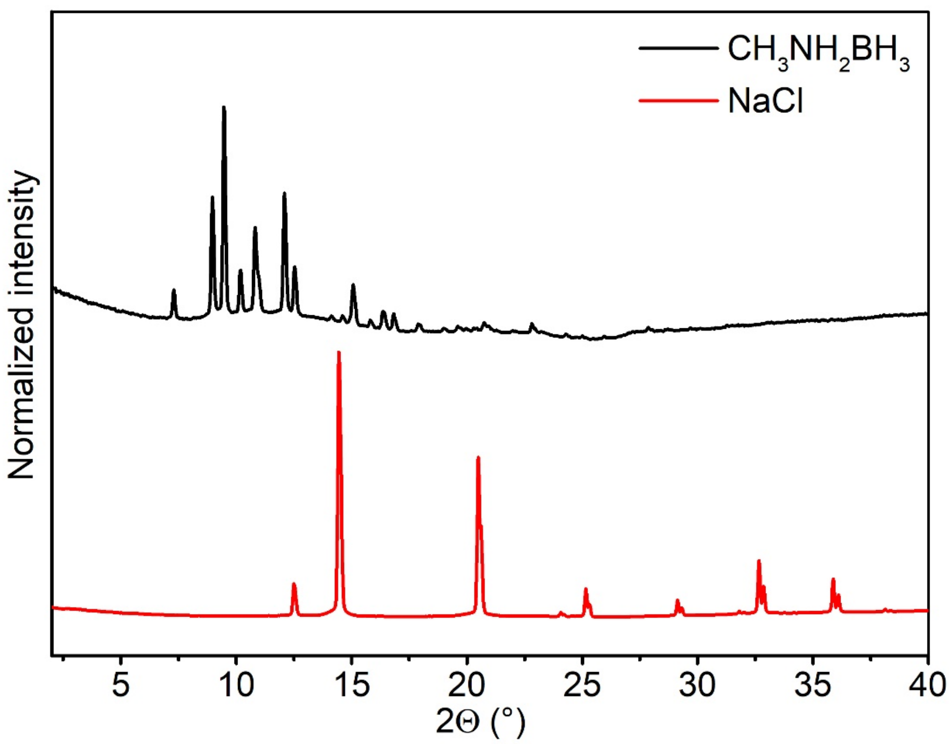

Fig. S4 PXRD pattern of $CH_3NH_2BH_3$ and NaCl

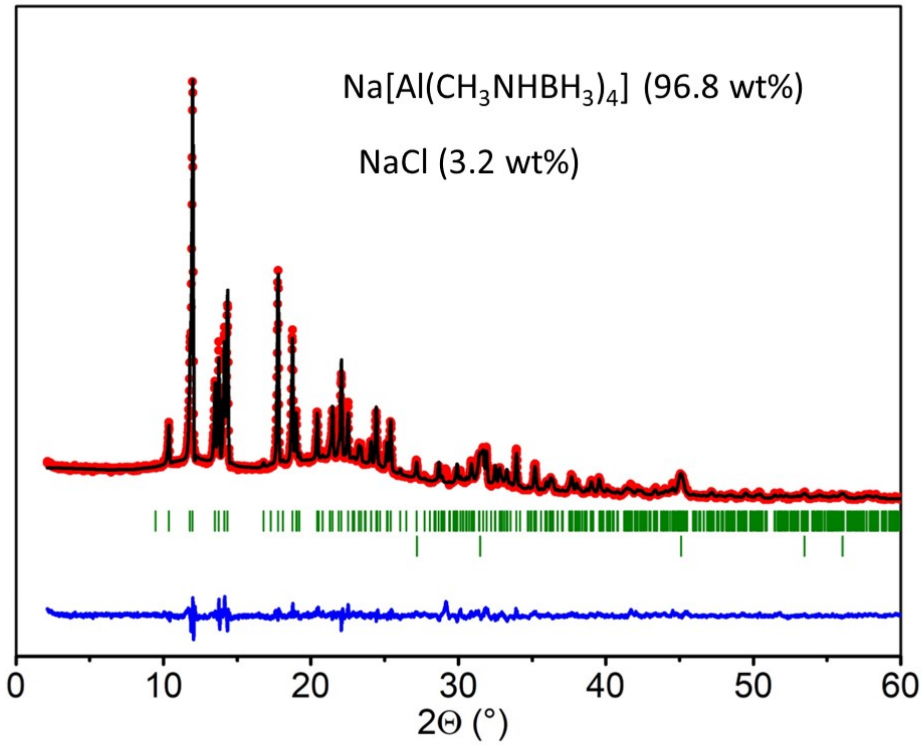

Fig. S5 Rietveld refinement of the HR-PXRD diffractogram of $NaAlH_4$- 4 $CH_3NH_2BH_3$ containing $Na[Al(CH_3NHBH_3)_4]$ (upper green marker), NaCl (lower green marker) (λ = 1.54056 Å). Observed data (Y_{obs}, red curve), Rietveld refinement profile (Y_{calc}, black curve), and difference plot (Y_{obs} - Y_{calc}, blue curve). Agreement factors, corrected for background, are R_{exp} = 9.41 %, R_{wp} = 16.3 %, R_p = 18.8%, χ^2 = 3.

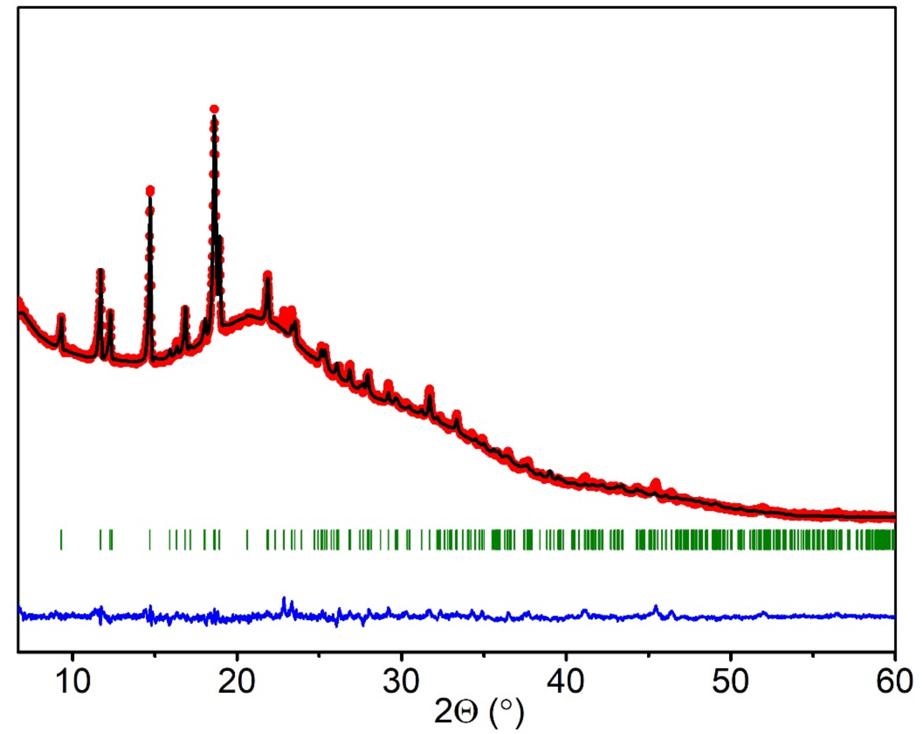

Fig. S6 Rietveld refinement of the HR-PXRD diffractogram of $Na[AlH(CH_3NHBH_3)_3]$ (λ = 1.54056 Å). Observed data (Yobs, red curve), Rietveld refinement profile (Ycalc, black curve), and difference plot (Yobs - Ycalc, blue curve). Agreement factors, corrected for background, are R_{exp} = 11.92 %, R_{wp} = 22.4 %, R_p = 38.3 %, χ2 = 3.52.

Table S1. Parameters used for the optimization of the synthesis of $Na[Al(CH_3NHBH_3)_4]$

Approach	Rotation speed (rpm)	Milling time(min)	Break time(min)	Number of cycles	Ball to powder mass ratio
A	600	3	5	≥90	60:1
B	600	3	5	120	30:1
C	500	3	2	200	60:1
D	250	3	2	240	60:1

Table S2. Milling conditions reported for the synthesis of $Na[Al(NH_2BH_3)_4]$ and used for the synthesis of the new $Na[Al(CH_3NHBH_3)_4]$ complex

Complex	Rotation speed (rpm)	Milling time(min)	Break time(min)	Number of cycles	Ball to powder mass ratio
$Na[Al(NH_2BH_3)_4]$	600	3	5	240	30:1
$Na[Al(CH_3NHBH_3)_4]$	600	3	5	120	30:1

Fig. S7 Photographs of product after different amounts of milling cycles based on Approach A.

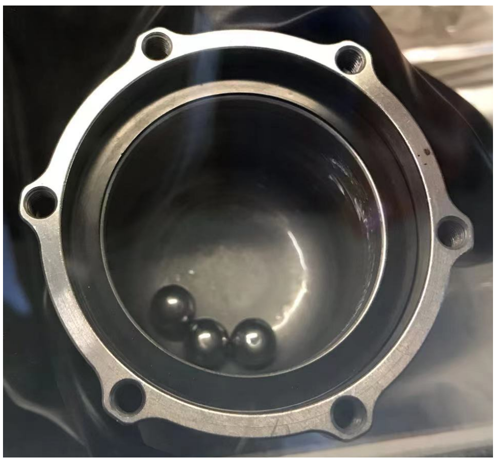

Fig. S8 Photograph of sample used for isolating the $Na[AlH(CH_3NHBH_3)_3]$ intermediate after 15 cycles of milling before drying.

Table S3. N-$H^{\delta+}$...$H^{\delta-}$-B bond lengths and N-H...H angles in $Na[Al(NH_2BH_3)_4]$, $Na[AlH(CH_3NHBH_3)_3]$ and $Na[Al(CH_3NHBH_3)_4]$ complexes.

Complex	N-$H^{\delta+}$...$H^{\delta-}$-B	D(H⋯H)/Å	∠(N-H⋯H)/ °
$Na[Al(NH_2BH_3)_4]$	N(1)-H(11) ...H(15)-B(1)	2.06	169.0
	N(1)-H(12) ...H(25)-B(2)	2.18	134.4
	N(2)-H(22) ...H(13)-B(1)	2.16	139.3
	N(3)-H(31) ...H(35)-B(3)	2.24	137.2
	N(3)-H(32) ...H(15)-B(1)	2.28	157.6
	N(4)-H(41) ...H(23)-B(2)	1.96	143.9
	N(4)-H(42) ...H(45)-B(4)	2.00	162.1
$Na[AlH(CH_3NHBH_3)_3]$	N(31)-H(31) ...H(01)-Al(1)	2.43	139.6
$Na[Al(CH_3NHBH_3)_4]$	N(21)-H(21) ...H(44)-B(41)	2.09	149.2
	N(31)-H(31) ...H(14)-B(11)	2.34	160.4
	N(41)-H(41) ...H(33)-B(31)	2.15	141.5
	N(41)-H(41) ...H(32)-B(31)	2.21	142.3

Table S4. B-N bond lengths in $CH_3NH_2BH_3$, $Na[AlH(CH_3NHBH_3)_3]$ and $Na[Al(CH_3NHBH_3)_4]$

	$CH_3NH_2BH_3$	$Na[AlH(CH_3NHBH_3)_3]$	$Na[Al(CH_3NHBH_3)_4]$
	1.58(7)	1.46(3)	1.57(1)
N-B(bond length)		1.54(2)	1.54(7)
		1.47(3)	1.52(7)
			1.57(0)

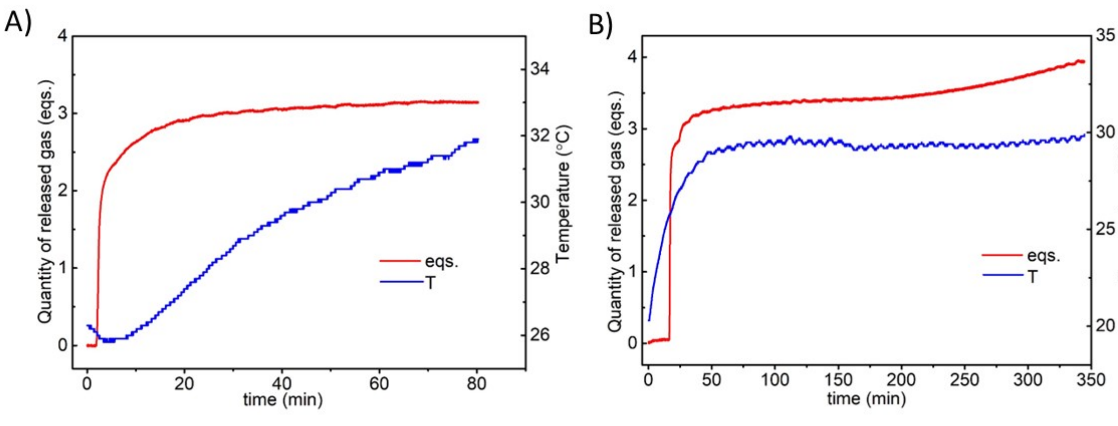

Fig. S9 The quantity of gas per Al released and temperature during the synthesis of $Na[AlH(CH_3NHBH_3)_3]$ (A) and $Na[Al(CH_3NHBH_3)_4]$ (B).

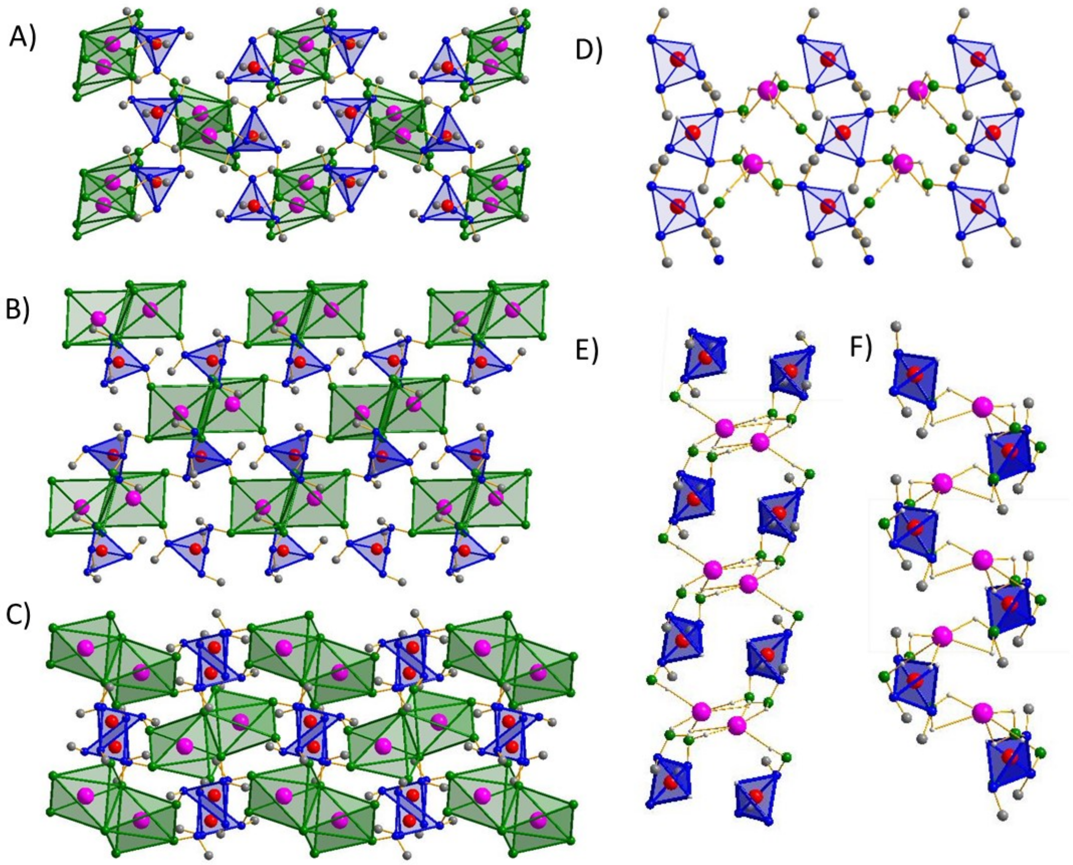

Fig. S10. Crystal packing of Al and Na coordination polyhedra in the structure of $Na[Al(CH_3NHBH_3)_4]$ and $Na[AlH(CH_3NHBH_3)_3]$ along the a (A,D), b (B,E), and c (C,F) axis. Color code: N = blue, B = green, C = grey, H = light grey, Al = red, and Na = pink. Hydrogen atoms are omitted for clarity.

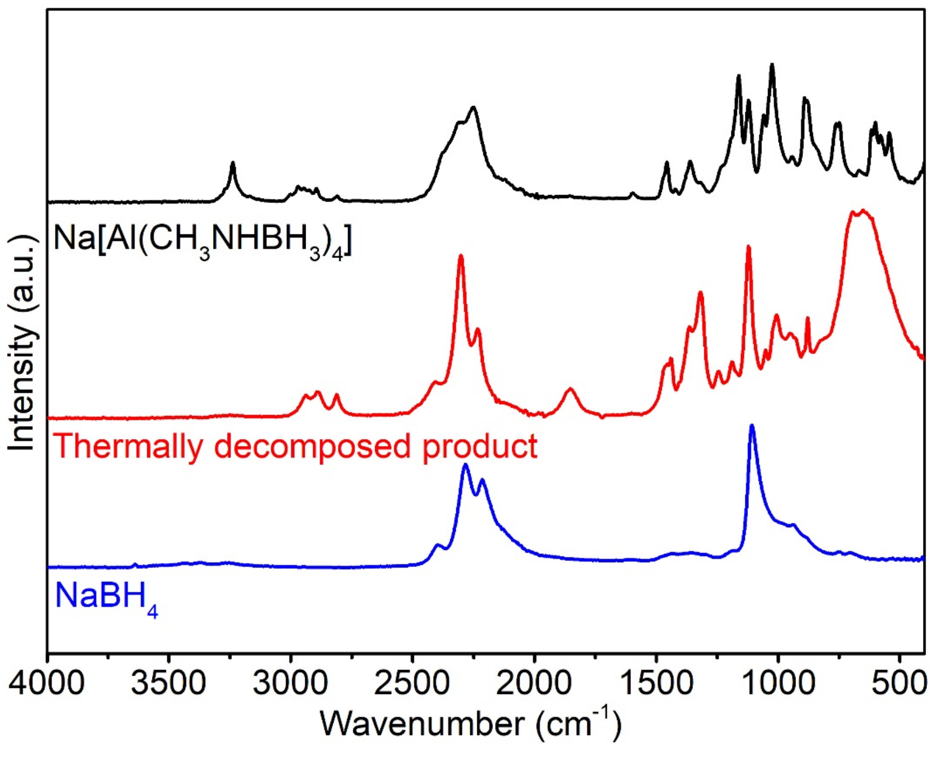

Fig. S11. ATR-IR spectra of $Na[Al(CH_3NHBH_3)_4]$, $NaBH_4$, and the residue obtained upon heating $Na[Al(CH_3NHBH_3)_4]$ at 100°C.

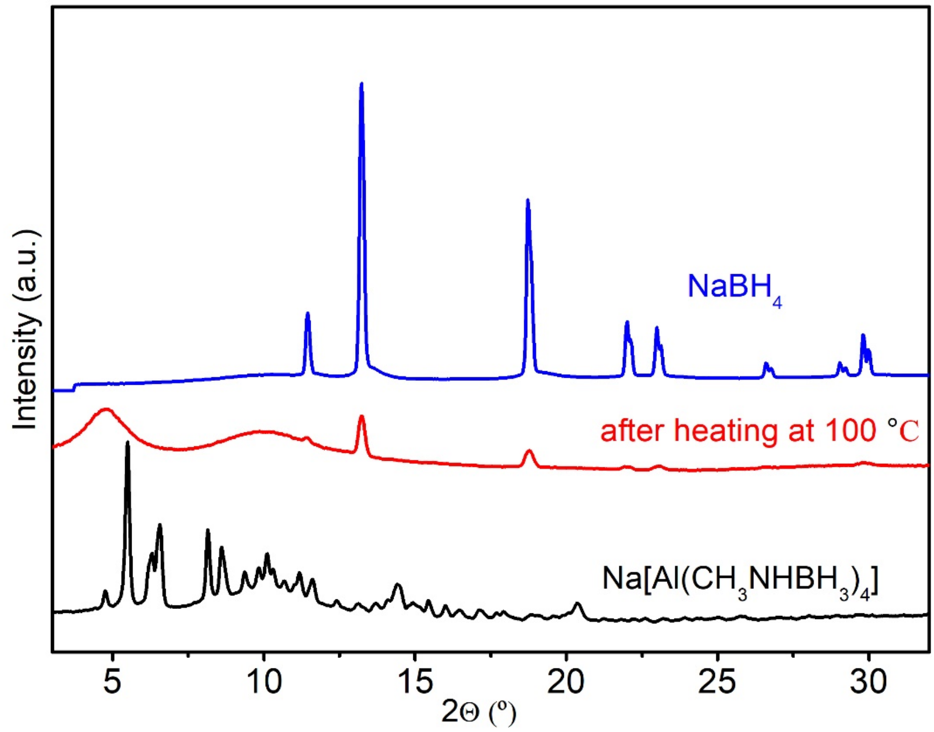

Fig. S12. PXRD patterns of $Na[Al(CH_3NHBH_3)_4]$, $NaBH_4$, and the residue obtained upon heating $Na[Al(CH_3NHBH_3)_4]$ at 100°C.

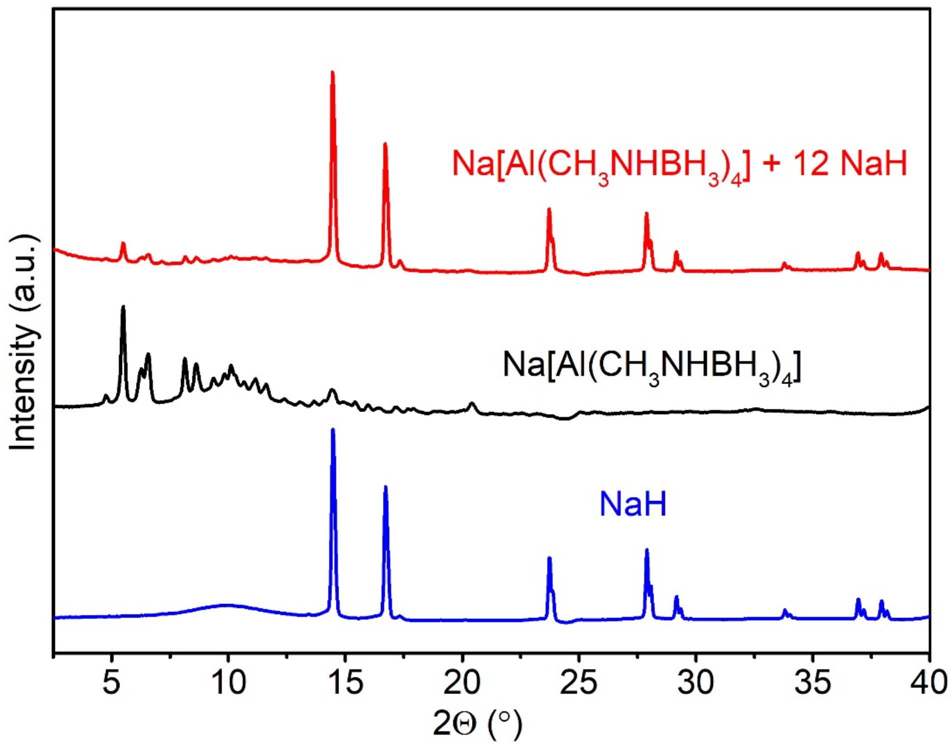

Fig. S13 PXRD patterns of $Na[Al(CH_3NHBH_3)_4]$+ 12 NaH, $Na[Al(CH_3NHBH_3)_4]$, and commercial NaH.

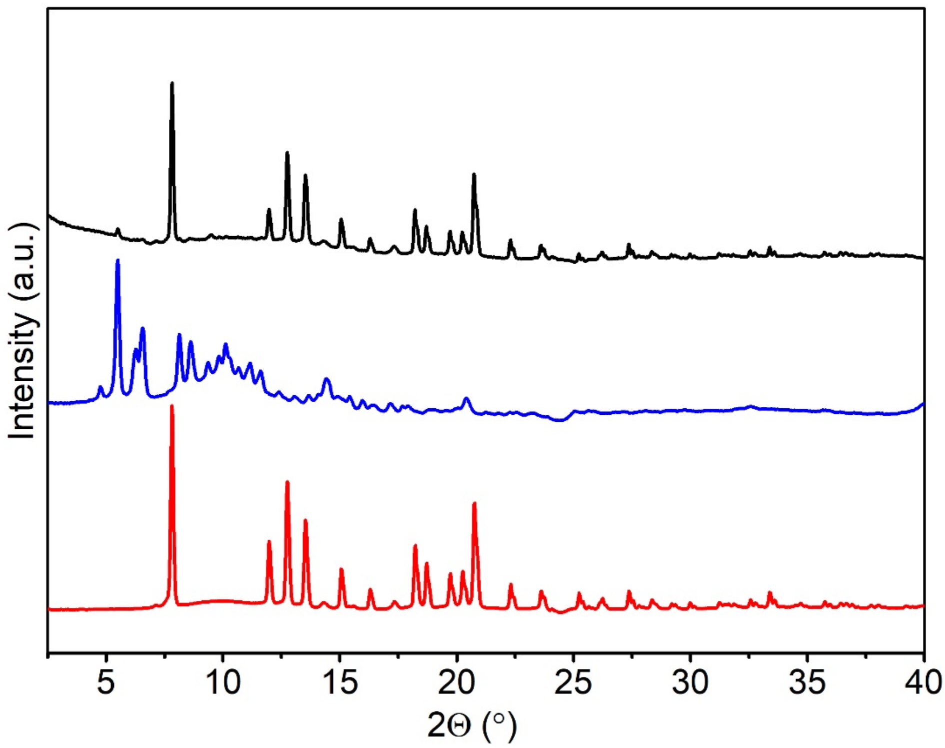

Fig. S14 PXRD patterns of Na[Al(CH_3NHBH_3)$_4$]+ 6 $NaNH_2$, Na[Al(CH_3NHBH_3)$_4$], and commercial $NaNH_2$.

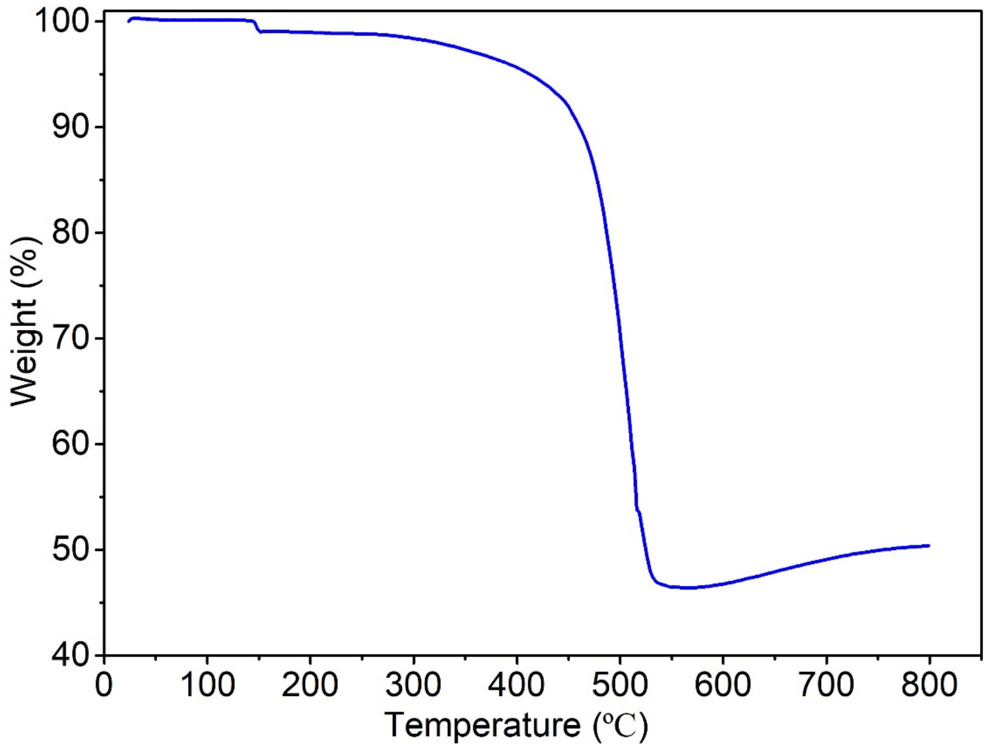

Figure S15. TGA curve of commercial $NaNH_2$.

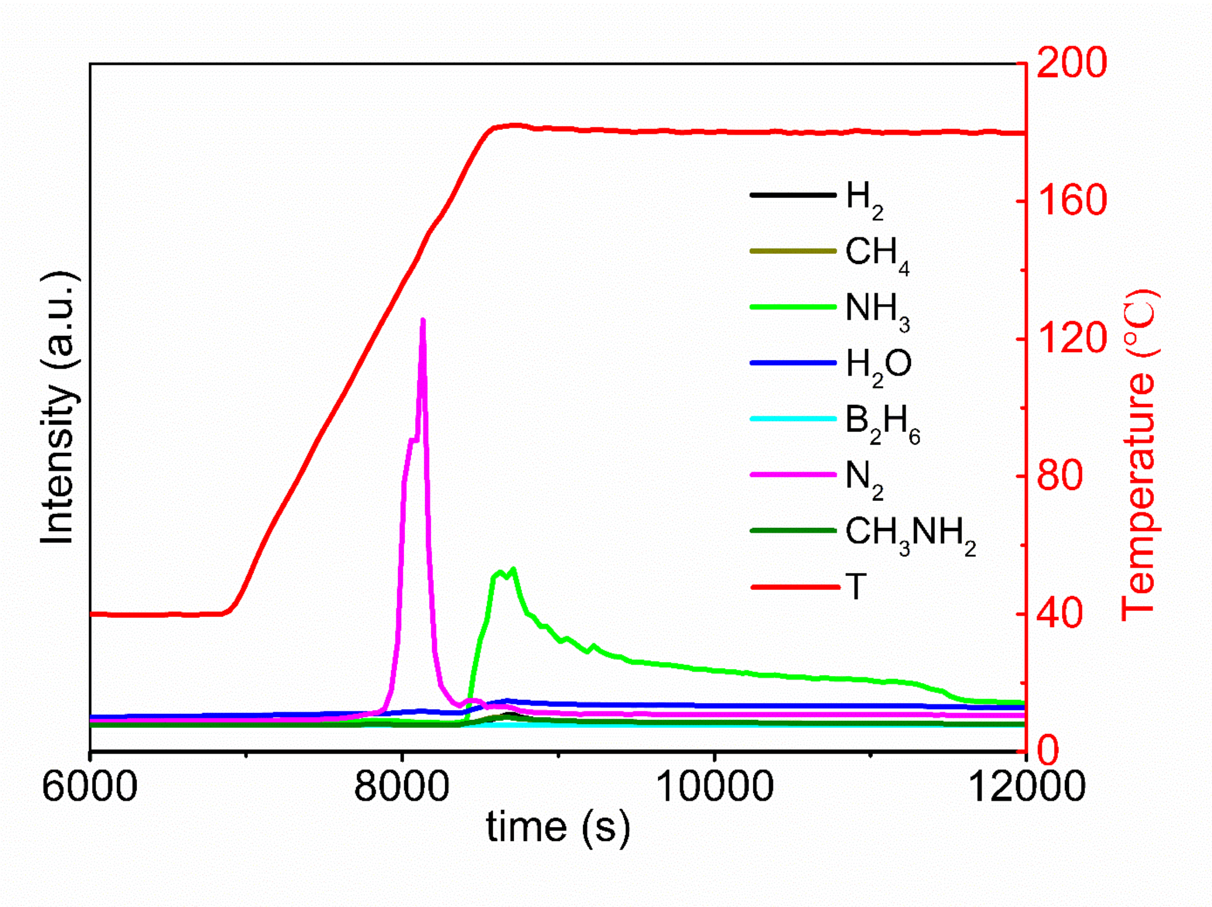

Fig. S16. MS spectra of commercial $NaNH_2$ corresponding to time.

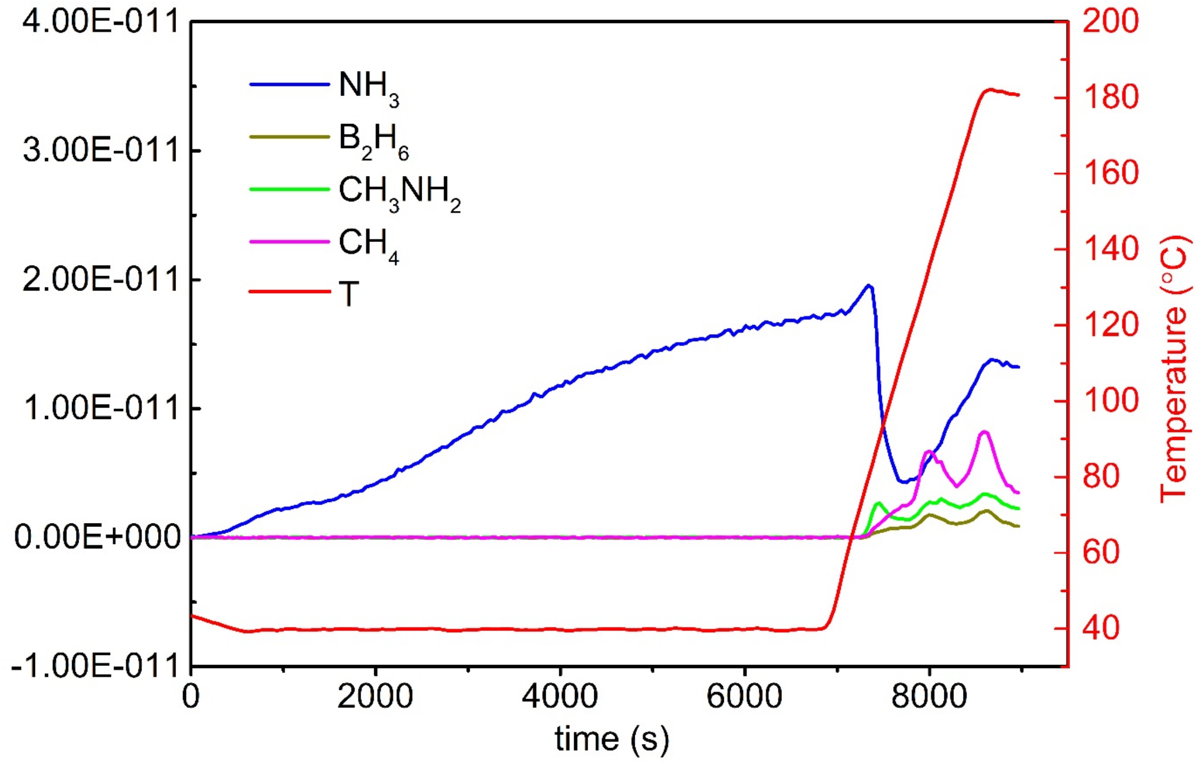

Fig. S17 Zoomed in the non-H_2 MS curve of $Na[Al(CH_3NHBH_3)_4]$ + 12 NaH

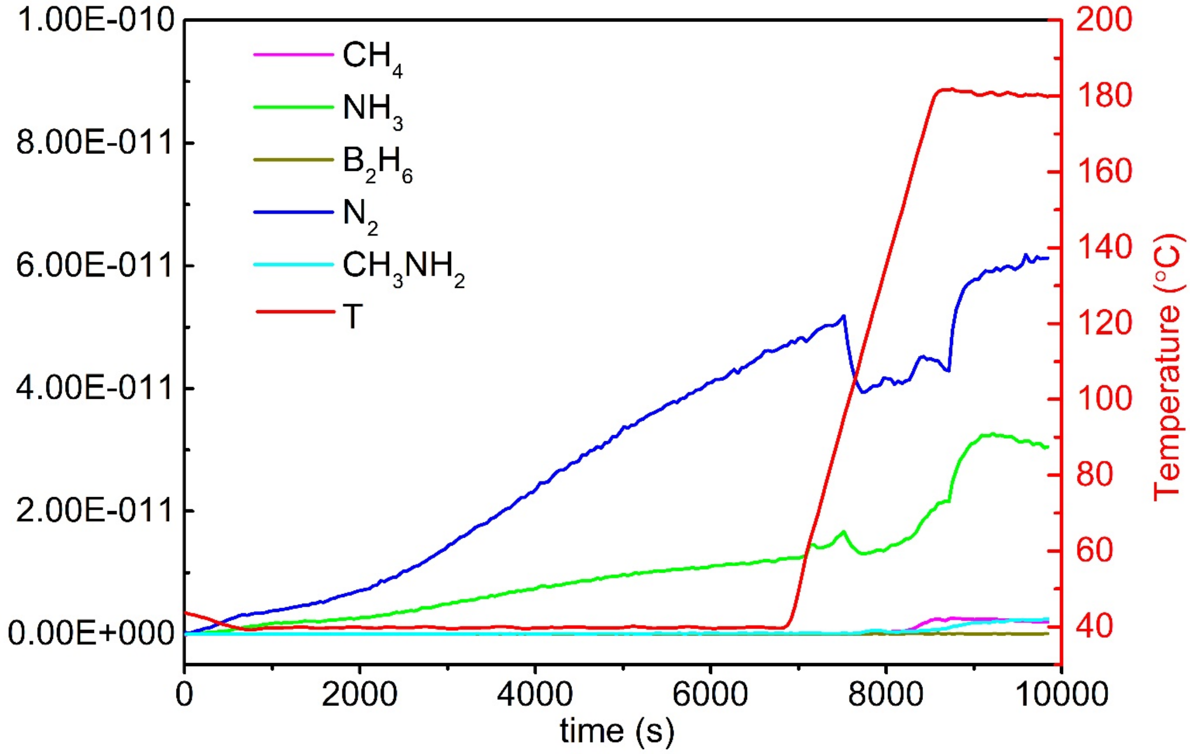

Fig. S18 Zoomed in the non-H_2 MS curve of $Na[Al(CH_3NHBH_3)_4]$ + 6 $NaNH_2$

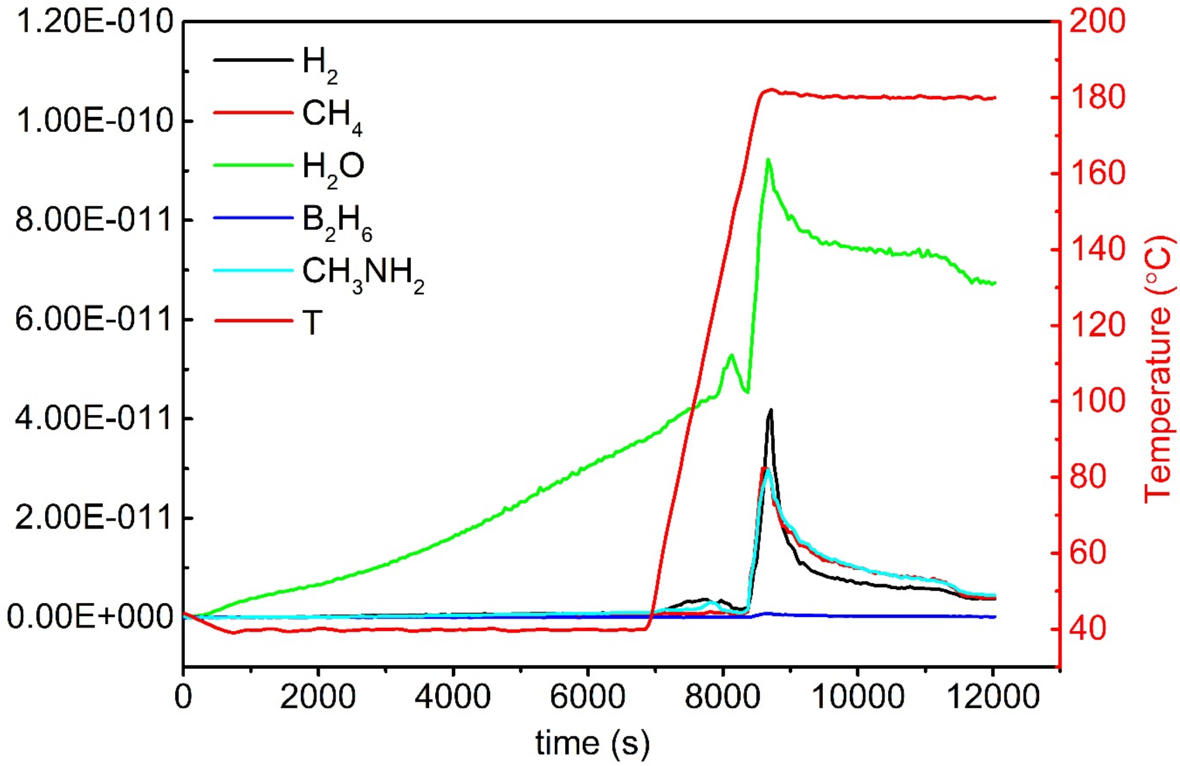

Fig. S19 Zoomed in the non-N_2 and NH_3 MS curve of commercial $NaNH_2$

Table S5. The molar mass, density, the molar volume and hydrogen densities of $Na[Al(CH_3NHBH_3)_4]$, NaH and $NaNH_2$ and their composites.

Compound	M (g/mole)	δ (g/cm^3)	V (cm^3)	Gravimetric density (%)	Volumetric density (g/l)
$Na[Al(CH_3NHBH_3)_4]$	225.5	1.014	222.4	12.42	126
NaH	24	1.47	16.3	4.17	61
$NaNH_2$	39	1.39	28.1	5.13	71
$Na[Al(CH_3NHBH_3)_4]$ + 12 NaH	513.5	-	418.3	7.79	96
$Na[Al(CH_3NHBH_3)_4]$ + 6 $NaNH_2$	459.5	-	390.7	8.70	102